**International Journal of Basic Science and Technology**
August, Volume 11, Number 3, Pages 229 - 239 http://www.ijbst.fuotuoke.edu.ng/ 229
https://doi.org/10.5281/zenodo.16871551 ISSN 2488-86

# Computational Insights into Corrosion Inhibition Efficiency of 5-Bromothiophene-2-Carbaldehyde: A DFT and Monte Carlo Simulation Approach

[1*]Badeji, A.A., [2]Luke, U.[3]Oladipo, S.D., [3]Adeleke, A.A. and [4]Louis, H
[1] Department of Chemical Sciences, Tai Solarin University of Education, Ijagun, Ogun State, Nigeria
[2] Department of Biochemistry, University of Uyo, Uyo, Nigeria
[3] Department of Chemical Sciences, Olabisi Onabanjo University, Ago-Iwoye, P.M.B. 2002, Nigeria
[4] Department of Pure and Applied Chemistry, University of Calabar, Calabar, Nigeria

**Article Information**

Article # 100284
Received: 8th May. 2025
1st Revision 19th May. 2025
2nd Revision:28th May 2025
Acceptance:29th July 2025
Available online:
10th August 2025.

**Keywords**
5-Bromothiophene-2-Carbaldehyde;
Monte Carlo simulation;
Corrosion inhibition;
Electrophilicity index
DFT

**Abstract**

This study investigates the corrosion inhibition efficiency of 5-Bromothiophene-2-Carbaldehyde (5-BTCA) using a combined Density Functional Theory (DFT) and Monte Carlo (MC) simulation approach. Quantum chemical calculations performed with Gaussian 16 evaluated the structural, electronic, and vibrational properties of 5-BTCA in the gas phase and in DMSO, ethanol, and water. Results reveal minimal solvent impact on molecular geometry but significant influence on vibrational frequencies, especially in polar solvents. The DFT calculations revealed 5-BTCA as a strong electron donor with a lower HOMO-LUMO energy gap (4.551 eV in $H_2O$ and 4.567 eV in ethanol), which signifies greater reactivity and absorptivity in the aqueous environment. The chemical potential ($\mu$ = -4.633 eV in $H_2O$) and electrophilicity index ($\omega$ = 4.714 in $H_2O$) indicated the molecule to be involved in strong interactions with metal surfaces. Natural Bond Orbital (NBO) analysis showed stable donor-acceptor interactions and solvent effects on $\pi$-bond delocalization. MC simulations, conducted on the Fe(110) surface in an acidic environment, demonstrate strong spontaneous adsorption of both protonated and unprotonated 5-BTCA, with the protonated form exhibiting slightly higher adsorption energy, indicating superior inhibition stability.

***Corresponding Author**: Badeji, A. A.; ogunlanaaa@tasued.edu.ng

## Introduction

Corrosion poses a serious threat in many industrial applications, causing the deterioration of metals and resulting in significant economic losses worldwide, estimated at over $2.5 trillion annually. Environmental factors such as moisture, oxygen, and aggressive ions like chloride and sulfate accelerate electrochemical degradation. This highlights the urgent need for effective corrosion mitigation strategies (Popoola *et al.* 2013, Prasad *et al.* 2020, Sheryazov *et al.* 2024). Organic corrosion inhibitors have gained attention as a sustainable, cost-effective, and eco-friendly alternative. These inhibitors commonly contain heteroatoms (N, O, S) or $\pi$-electron-rich structures that adsorb onto metal surfaces, forming protective layers that prevent corrosive agents from attacking the metal (Aliofkhazraei 2018, Al-Amiery *et al.* 2023, Al-Amiery *et al.* 2024, Roscher *et al.* 2024). Computational and surface chemistry methods often complement experimental studies to better understand corrosion inhibition, focusing on electron density distribution, molecular orbital interactions, and charge transfer processes that influence inhibitor adsorption and efficiencies (Verma *et al.* 2017, Ueda 2022, Akrom 2024, Gaber *et al.* 2024, Kumar *et al.* 2024).

Among organic inhibitors, thiophene derivatives have gained significant attention due to their unique electronic and structural properties (Guo *et al.* 2018, Arrousse *et al.* 2022, Resen *et al.* 2023). One of such compound is 5-Bromothiophene-2-Carbaldehyde (5-BTCA), featuring a thiophene ring substituted with bromine and aldehyde groups (*Figure 1*), making it a promising candidate for corrosion inhibition (Arrousse *et al.* 2022). While the bromine atom enhances charge transfer due to its high polarizability (Guo *et al.* 2018, Resen *et al.* 2023), the thiophene ring supports $\pi$-electron interactions with metal surfaces, and the electron-withdrawing aldehyde group increases electron density on the ring, facilitating chemisorption with metal *d*-orbitals like those of iron and steel (Resen *et al.* 2023). These combined effects enable 5-BTCA to form dense, stable protective layers that significantly reduce corrosion rates under challenging

https://doi.org/10.5281/zenodo.16871551 ISSN 2488-86

conditions (Guo *et al.* 2018, Arrousse *et al.* 2022, Resen *et al.* 2023).

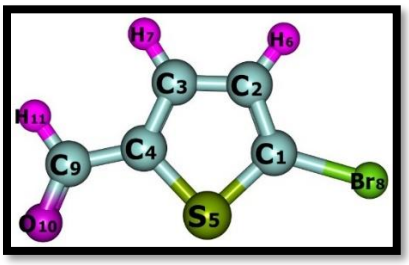


Figure 1. 3D structure of 5-bromothiophene-2-carbaldehyde (5-BTCA).

To investigate the molecular mechanism underlying the efficacy of 5-BTCA, the present study uses a combined density functional theory (DFT) and Monte Carlo (MC) simulation (Singh *et al.* 2019) to obtain information on the adsorption behaviour and reactivity of 5-BTCA and get the prediction of the most favourable adsorption configurations and also the calculation of adsorption energies of 5-BTCA on metal surfaces under varying conditions (Shaker *et al.* 2024).

**Computational details**

**DFT calculations:** Quantum chemical investigations of 5-BTCA were conducted using DFT via Gaussian 16 program package (Frisch 2016) to study its structural and electronic properties. Geometry optimizations were performed in the gas phase and solvents (DMSO, water, ethanol) to analyze solvent effects, employing the B3LYP hybrid functional known for accurately representing electronic structures (Becke 1993, Zhao *et al.* 2005, Gece 2008) combined with the correlation-consistent polarized valence triple-zeta (cc-pVTZ) basis set for a balance of accuracy and computational efficiency (Dunning Jr 1989, Wilson *et al.* 1999). The basis set was selected as a good compromise between accuracy and the computational costs to describe the electronic distributions in space during the calculations. Solvent influences were modelled with the SMD implicit solvation model in conjunction with the self-consistent reaction field (SCRF) method (Marenich *et al.* 2009). Vibrational frequency calculations confirmed optimized structures as minimal by showing no imaginary frequencies (Fukui 1981). Reactivity was assessed using Molecular Electrostatic Potential (MESP) maps that visualize charge distribution, highlighting nucleophilic and electrophilic regions (Liu *et al.* 2018, Suresh *et al.* 2022, Badeji *et al.* 2024). Frontier Molecular Orbital (FMO) theory analyzed HOMO and LUMO energies and their gap (ΔE), where a smaller energy gap indicates higher reactivity. Key global reactivity descriptors, including hardness (η), softness (σ), electronegativity (χ), and electrophilicity index (ω), were computed to quantify molecular stability and electron-transfer abilities, providing insights into how 5-BTCA interacts chemically in various environments (Fukui *et al.* 1952, Zhan *et al.* 2003, Huang *et al.* 2017, Oladipo *et al.* 2025). This comprehensive approach allows for elucidation of the molecule's electronic behaviour relevant to its corrosion inhibition potential.

*2.2. Monte Carlo Simulation*

This study employed Monte Carlo (MC) and molecular dynamics (MD) simulations using the Materials Studio 2017 software suite (Hansen 2018, Shankar *et al.* 2022) to investigate the adsorption of 5-BTCA on the Fe(110) iron surface in an acidic environment. The Fe(110) surface, relevant to the mild steel industry, was modelled as a 10 × 10 supercell slab optimized with the COMPASS II force field. The optimized slab was enlarged to a 10 × 10 supercell and placed in a simulation box (24.8 × 24.8 × 38.1 Å³) with 30 Å of vacuum along the z-axis to limit periodic boundary effects. The molecular geometry of 5-BTCA was also minimized with stringent convergence criteria with the Forcite module and with the COMPASS II force field to explicitly consider polar and heteroatom interactions (Akinyele *et al.* 2022, Oyeneyin *et al.* 2022, Oyeneyin *et al.* 2024). MC simulations identified optimal adsorption configurations, allowing 5-BTCA freedom to move over a fixed iron surface. Simulated annealing explored adsorption energy landscapes, while parameters such as total energy, adsorption energy, and deformation energy quantified binding strength and stability. This integrated approach combined structural optimization, configurational sampling, and dynamic behaviour analysis to effectively model the strong, spontaneous adsorption of 5-BTCA on Fe(110), validating its corrosion inhibition mechanism under acidic conditions.

**Results and discussion**

**Geometry optimization**

5-Bromothiophene-2-carbaldehyde (5-BTCA) is a five-membered heterocyclic compound featuring functional groups such as carbonyl (C=O), carbon-carbon double bond (C=C), carbon–bromine (C–Br), carbon-hydrogen (C–H), and carbon-sulfur (C–S) bonds, as shown in *Figure 1*. Its structure consists of a thiophene ring substituted with a carbaldehyde group at the 2-position and bromine at the 5-position. Density Functional Theory (DFT) calculations optimized the molecular geometry in the gas phase and in solvents: DMSO, ethanol, and water. The optimized

structures revealed that the bond lengths varied very little among different environments and the various polarities of the solvents, indicating that solvent polarity had little impact on the molecular geometry of 5-BTCA (*Table 1*). For example, the Br-C bond length remained consistently 1.89 Å, and the C-S bond length ranged narrowly from 1.74 to 1.75 Å (Mouats *et al.* 2024). Slight changes occurred in the C=C and C=O bonds, with ethanol inducing minor contraction or elongation, possibly due to intermolecular interactions. Overall, these findings reflect the structural stability of 5-BTCA under varying conditions and indicate only slight solvent influence on specific bonds, particularly with the C=O and C=C bonds. The similarity observed in most bond lengths suggests the structural stability of 5-BTCA across diverse conditions.

Table 1. Bond lengths of 5-bromothiophene-2-carbaldehyde (5-BTCA) in different solvents

| Compounds | Br-C (A) | C-S (A) | C=C (A) | C=O (A) | C-H (A) |
|---|---|---|---|---|---|
| 5-BTCA-DMSO | 1.89 | 1.75 | 1.37 | 1.22 | 1.10 |
| 5-BTCA-ethanol | 1.89 | 1.74 | 1.37 | 1.21 | 1.11 |
| 5-BTCA-$H_2O$ | 1.89 | 1.75 | 1.38 | 1.22 | 1.10 |
| 5-BTCA- Gas | 1.89 | 1.75 | 1.38 | 1.22 | 1.10 |

**Vibrational Analysis:** Vibrational studies of 5-BTCA revealed significant solvent effects on its molecular vibrations, especially in polar solvents (DMSO, ethanol, $H_2O$) compared to the gas phase. The symmetric CH=CH stretching frequency remained mostly unchanged, indicating minimal solvent impact, while the asymmetric CH=CH stretching showed slight variations, with $H_2O$ causing a stiffer C=C bond (Table 2). Larger shifts occurred in the symmetric CH and C=O stretches, where $H_2O$ induced the highest CH frequency (2970.24 $cm^{-1}$) and the lowest C=O frequency (1663.55 $cm^{-1}$), reflecting strong solvent interactions that weaken the carbonyl and stiffen the CH bond (Nyquist 1986). Minor shifts in C=C scissoring and CH=CH rocking vibrations also occurred. The symmetric C-S stretching frequency was relatively stable but slightly higher in the gas phase (Šebek *et al.* 2013). Overall, polar solvents cause frequency shifts indicating reduced bond strengths due to solvation, while the gas phase exhibits stronger, more stable bonds.

Table 2. Frequencies of 5-bromothiophene-2-carbaldehyde (5-BTCA) and vibrational modes in different solvents

| Assignments | 5-BTCA -DMSO ($cm^{-1}$) | 5-BTCA -ethanol ($cm^{-1}$) | 5-BTCA -$H_2O$ ($cm^{-1}$) | 5-BTCA -Gas ($cm^{-1}$) |
|---|---|---|---|---|
| Symmetric CH=CH | 3227.70 | 3227.47 | 3232.21 | 3225.49 |
| Asymmetric CH=CH | 3207.66 | 3207.70 | 3212.57 | 3196.50 |
| Symmetric CH | 2936.77 | 2956.74 | 2970.24 | 2884.50 |
| Symmetric C=O | 1718.73 | 1687.33 | 1663.55 | 1750.52 |
| Scissoring C=C | 1450.42, 1415.99, 1333.86 | 1448.61, 1413.20, 1333.38 | 1447.62, 1411.08, 1333.02 | 1450.61, 1413.10, 1332.75 |
| Rocking CH=CH | 1566.38, 1237.59, 1227.96 | 1564.77, 1238.53, 1235.31 | 1563.68, 1240.61, 1236.14 | 1565.18, 1235.78, 1224.32 |
| Symmetric C-S | 679.79, 652.88 | 680.09, 654.09 | 679.90, 653.42 | 684.05, 658.59 |

**Quantum Chemical Analysis**: Quantum chemical descriptors from DFT calculations provide useful insights into the corrosion inhibition performance of 5-BTCA in different media (Zhan *et al.* 2003, Huang *et al.* 2017, Badeji *et al.* 2024). The descriptors related to the corrosion inhibition performance of 5-BTCA are presented in *Table 3* and *Figures 2 and 3*. Among solvents studied (DMSO, ethanol, water, and gas phase), the highest IP was observed in the gas phase (7.039 eV), indicating lower electron donation, while 5-BTCA in water showed a lower IP (6.908 eV), suggesting enhanced electron-donating ability that facilitates adsorption on metal surfaces. The smaller HOMO-LUMO energy gaps in ethanol (4.567 eV) and water (4.551 eV) signify increased chemical reactivity and better interaction with metals, boosting inhibition

https://doi.org/10.5281/zenodo.16871551 ISSN 2488-86

efficiency. Additionally, the electrophilicity index was higher in ethanol and water, indicating stronger electron-accepting capabilities. Lower hardness and higher softness values in these aqueous media reflect improved adsorption potential and molecular reactivity. The more negative chemical potentials in water (-4.633 eV) and ethanol (-4.613 eV) further indicate a greater tendency for electron donation, aiding adsorption. These electronic properties collectively affirm that 5-BTCA exhibits superior corrosion inhibition in aqueous environments (Oladipo *et al.* 2023). The theoretical findings provide strong support for the practical application of 5-BTCA as an effective corrosion inhibitor, particularly in polar solvents.

Figure 2. Graphical representation of the quantum chemical descriptors for the studied 5-BTCA system on different solventedia.

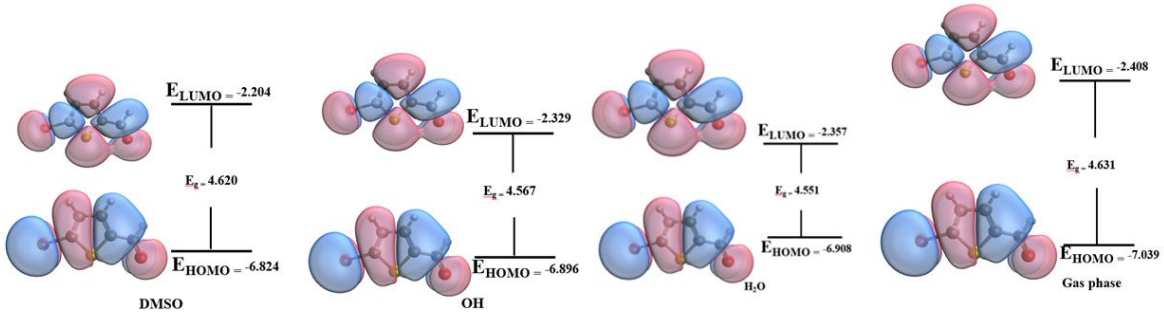


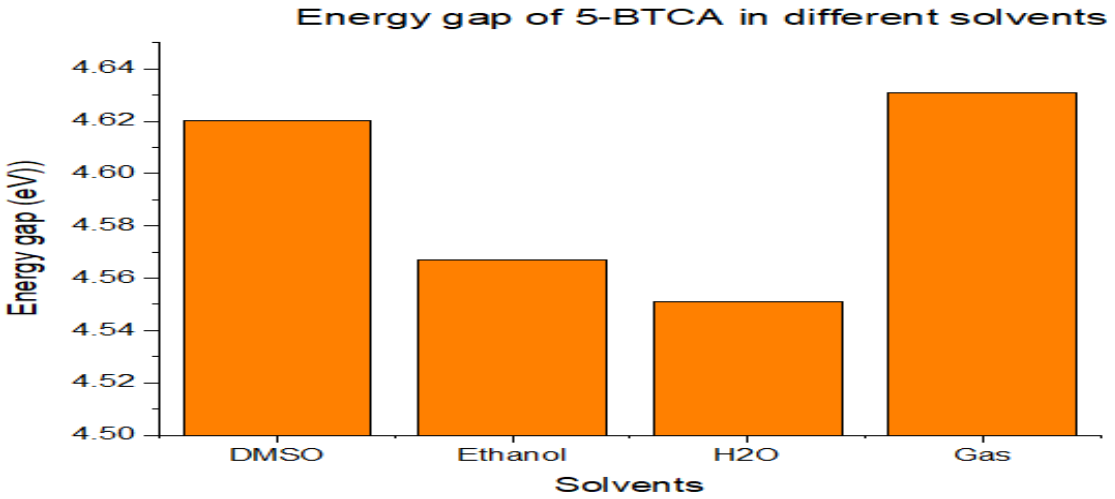


Figure 3. Fluctuation of the Energy Gap (**Eg**) for 5-Bromothiophene-2-Carbaldehyde (5-BTCA) in Different Solvent Media.

The plot illustrates variations in the HOMO-LUMO energy gap across different environments, highlighting the influence of solvent polarity on the electronic properties of 5-BTCA.

*Table 3.* Theoretically calculated quantum descriptor parameters for the investigated 5-bromothiophene-2-carbaldehyde (5-BTCA) complex in different solvent media.

| Modelled Systems | IP/eV | EA (eV) | χ (eV) | HOMO/eV | LUMO/eV | $E_g$ (eV) | ω (eV) | η (eV) | μ (eV) | S (eV) |
|---|---|---|---|---|---|---|---|---|---|---|

| | | | | | | | | | | |
|---|---|---|---|---|---|---|---|---|---|---|
| 5-BTCA-DMSO | 6.824 | 2.204 | -2.310 | -6.824 | -2.204 | 4.620 | 4.410 | 2.310 | 4.514 | 0.227 |
| 5-BTCA-Ethanol | 6.896 | 2.329 | -2.284 | -6.896 | -2.329 | 4.567 | 4.658 | 2.284 | 4.613 | 0.437 |
| 5-BTCA-$H_2O$ | 6.908 | 2.357 | -2.276 | -6.908 | -2.357 | 4.551 | 4.714 | 2.276 | 4.633 | 0.439 |
| 5-BTCA-Gas | 7.039 | 2.408 | -2.316 | -7.039 | -2.408 | 4.631 | 4.818 | 2.316 | 4.724 | 0.431 |

**Natural bond orbital (NBO) studies:** NBO analysis of 5-BTCA (*Table 4*) revealed solvent-dependent variations in donor-acceptor interactions, especially between polar solvents (DMSO, ethanol, water) and the gas phase. The $\pi C_1–C_2 \rightarrow \pi C_3–C_4$ interaction showed consistently high perturbation energies ($E^2$) across all environments, with the highest energy in the gas phase (120.35 kcal/mol) due to less solvent disturbance (Hasanzadeh 2024). In polar solvents like ethanol and water, these energies were slightly lower (~98.5 kcal/mol), indicating stabilization of the π-bonds by solvent effects. The $\pi C_3–C_4 \rightarrow \pi C_9–O_{10}$ interaction exhibited low $E^2$ values overall, with minor differences between the water (-18.56 kcal/mol) and gas phase (-16.78 kcal/mol), suggesting weak interactions. The perturbation energy differences *($E_{(j)}–E_{(i)}$) and coupling constants ($F_{(i,j)}$)* showed a similar trend across the environmental conditions, with negligible changes, indicating that the orbital overlaps across all media are stable (Mahmood *et al.* 2022). In summary, these results amplify the effect of solvent polarity in the stabilization and delocalization of π and π-bonds.

Table 4. Perturbation energies ($E^2$ kcal/mol), interaction types, energy differences ($E_{(j)}$-$E_{(i)}$) and coupling constant ($F_{(i,j)}$) of 5-bromothiophene-2-carbaldehyde (5-BTCA)

| Compounds | Donor (i) | Acceptor (j) | $E^2$ (kcal/mol) | $E_{(j)}$-$E_{(i)}$ | $F_{(i,j)}$ |
|---|---|---|---|---|---|
| 5-BTCA-DMSO | $\pi^*C_1$ - $C_2$ | $\pi^*C_3$ - $C_4$ | 92.95 | 0.01 | 0.061 |
| | $\pi C_3$ - $C_4$ | $\pi^*C_9$ - $O_{10}$ | 17.51 | 0.27 | 0.062 |
| 5-BTC-Ethanol | $\pi^*C_1$ - $C_2$ | $\pi^*C_3$ - $C_4$ | 98.60 | 0.01 | 0.061 |
| | $\pi C_3$ - $C_4$ | $\pi^*C_9$ - $O_{10}$ | 18.29 | 0.27 | 0.063 |
| 5-BTCA-$H_2O$ | $\pi^*C_1$ - $C_2$ | $\pi^*C_3$ - $C_4$ | 98.51 | 0.01 | 0.061 |
| | $\pi C_3$ - $C_4$ | $\pi^*C_9$ - $O_{10}$ | 18.56 | 0.27 | 0.064 |
| 5-BTCA-Gas | $\pi^*C_1$ - $C_2$ | $\pi^*C_3$ - $C_4$ | 120.35 | 0.01 | 0.060 |
| | $\pi C_3$ - $C_4$ | $\pi^*C_9$ - $O_{10}$ | 16.78 | 0.28 | 0.061 |

**Molecular Electrostatic Potential Analysis (MESP)** The Molecular Electrostatic Potential (MESP) of 5-BTCA was examined across different solvents, revealing visually similar plots but distinct electronic behaviours quantified by the electrophilicity index (ω) (*Figure 4*). In the gas phase, 5-BTCA has the highest ω (4.819 eV), indicating strong electrophilic reactivity due to lack of solvent stabilization (Gadre *et al.* 2021). In contrast, DMSO, a polar solvent, shows the lowest ω (4.393 eV), reflecting tight stabilization of electron density and reduced reactivity. Ethanol (ω=4.660 eV) and water (ω=4.715 eV) provide moderate stabilization, with ω values between those of the gas phase and DMSO, due to their hydroxyl groups partially stabilizing 5-BTCA's electronic structure. In spite of the similarity in the MESP plots shown below, there exist some subtle changes in the electron potential distribution. For example, there was a subtle difference in the electron density around Br and S atoms across all media due to solvent interaction; however, this might not be obvious. Overall, DMSO offers the strongest electronic stabilization, reducing electrophilicity, while ethanol and water allow moderate reactivity. Thus, the electrophilicity index effectively quantifies solvent effects on 5-BTCA's electronic properties, despite similar MESP appearances, highlighting that solvent polarity modulates its reactivity from highly reactive in nonpolar conditions to more stabilized in polar solvents.

https://doi.org/10.5281/zenodo.16871551 ISSN 2488-86

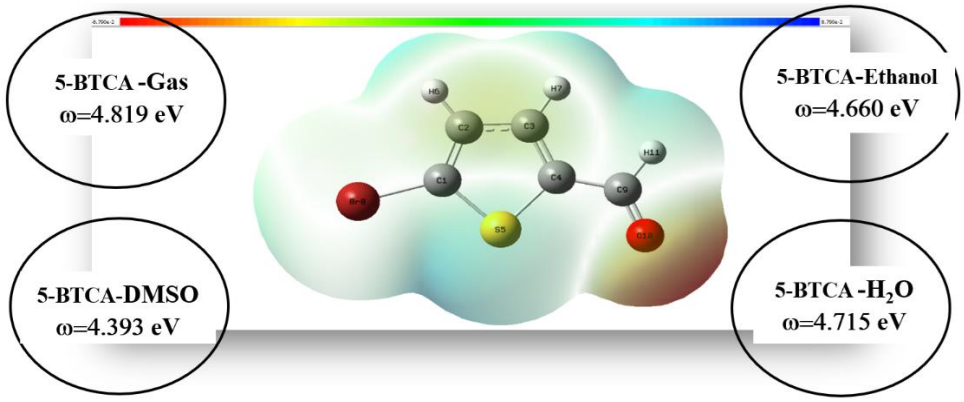


Figure 4. Pictorial representation of the molecular electrostatic potential iso-surface for 5-bromothiophene-2-carbaldehyde (5-BTCA) on different solvent media

**Monte Carlo Simulation**

The Monte Carlo simulation provides valuable insights into the adsorption behaviour of 5-BTCA on metal surfaces, clarifying its corrosion inhibition mechanism (Neyts and Bogaerts 2012, Hansen 2018). Key parameters include total energy ($E_{tot}$), where more negative values indicate a stable inhibitor-metal system; adsorption energy ($E_{ad}$), with negative values signifying strong, spontaneous adsorption crucial for corrosion protection; deformation energy ($E_{Def}$), reflecting structural changes upon adsorption, where lower values are favourable; and rigid adsorption energy ($E_{rig\_ad}$), measuring adsorption without structural flexibility. Both protonated 5-BTCA and unprotonated (5-BTCAH$^+$) were simulated in an acidic medium containing 50 water molecules, 10 hydronium ions ($H_3O^+$), and 10 chloride ions ($Cl^-$) on the Fe(110) crystallographic plane, a well-studied iron surface. The simulations as shown in *Table 5* and *Figure 5* provide clarity into the corrosion inhibition whereby 5-BTCA inhibits iron surfaces. The protonated 5-BTCAH$^+$ system showed a total energy of -3091.34 kcal/mol and a strong adsorption energy of -3105.63 kcal/mol, indicating stable and spontaneous binding despite limited structural flexibility. Its deformation energy of 72.90 kcal/mol suggests moderate structural adjustment, acceptable for efficient inhibition. Negative differential adsorption energies for the inhibitor, water, hydronium, and chloride ions demonstrate favourable interactions. The differential adsorption energy ($dE_{ad}/d_{Ni}$) for the inhibitor, $H_2O$, hydroxonium and the chloride ion are -74.31, -13.58, -143.80 and -142.86 kcal/mol, respectively. This implies that the protonated inhibitor can effectively compete with corrosive species for adsorption sites, maintaining a protective film on the metal surface and enhancing corrosion resistance.

Table 5. Monte Carlo simulation of adsorption of 5-BTCA species on Fe(110) in hydrochloric acid medium ($50H_2O/10H_3O^+/10Cl^-$)

| Systems | $E_{tot}$ (kcal/mol) | $E_{ad}$ (kcal/mol) | $E_{rigid\_ad}$ (kcal/mol) | $E_{Def}$ (kcal/mol) | $Inhibitor: dE_{ad}/d_{Ni}$ (kcal/mol) | $E_{bin}$ (kcal/mol) |
|---|---|---|---|---|---|---|
| Protonated | -3091.34 | -3105.63 | -3178.53 | 72.90 | -74.31 | -2716.80 |
| Unprotonated | -3104.60 | -3105.01 | -3177.42 | 72.41 | -86.17 | -2713.93 |

Parameters: $E_{tot}$: Total energy; $E_{ad}$: adsorption energy; $E_{rigid\_ad}$: rigid adsorption energy; $dE_{ad}/d_{Ni}$: differential adsorption energy

The unprotonated form of 5-BTCA exhibits a total energy of -3104.60 kcal/mol, slightly lower than the protonated form, with a strong adsorption energy of -3105.01 kcal/mol, indicating spontaneous binding to the metal surface. Its rigid adsorption energy (-3177.42 kcal/mol) and deformation energy (72.41 kcal/mol) closely resemble those of the protonated form, suggesting comparable adsorption strength and structural flexibility. Interaction energies with water (-13.58 kcal/mol), $H_3O^+$ (-143.80 kcal/mol), and $Cl^-$ (-142.86 kcal/mol) demonstrate strong electron interactions in acidic environments, implying competitive adsorption. The thiophene–Fe interaction yields –74.31 kcal/mol, while the $dE_{ad}/d_{Ni}$ value in the

https://doi.org/10.5281/zenodo.16871551 ISSN 2488-86

water phase is –13.58 kcal/mol, showing minimal deviation, suggesting that water does not significantly compete for adsorption. Moreover, the values for $H_3O^+$ (–143.80 kcal/mol) and $Cl^-$ (–142.86 kcal/mol) indicate strong electron interactions with charged species, which could imply competitive adsorption under acidic or chloride-rich conditions. Despite the presence of corrosive species, 5-BTCA's strong adsorption limits their access to the iron surface, reducing corrosion risk. Since protonated species dominate in acidic media, they likely enhance the molecule's affinity to metal through stronger electrostatic attraction.

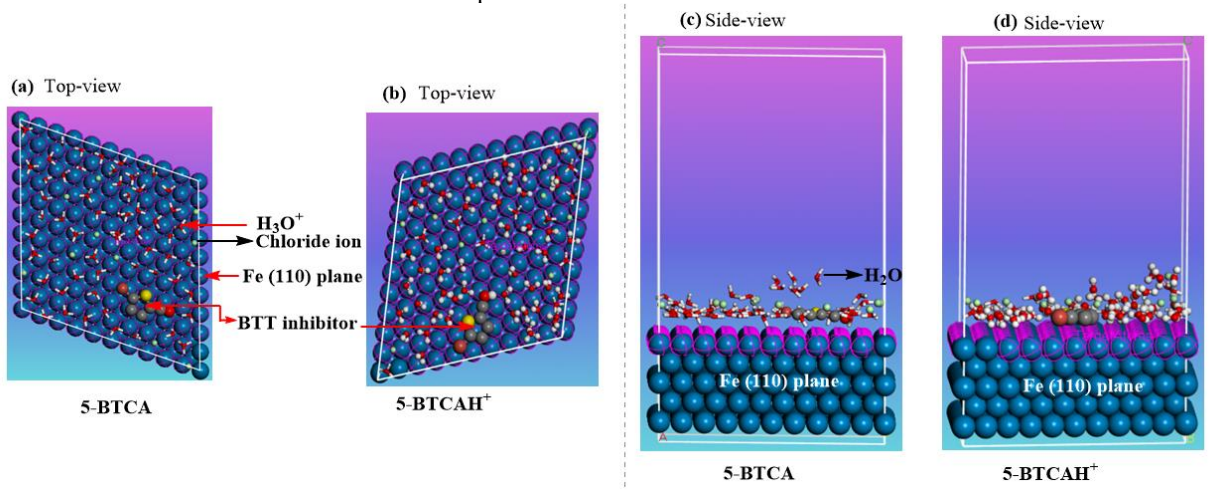


Figure 5. MD simulation for the adsorption of the inhibitor (5-BTCA) and its protonated form on Fe(110) surface in hydrochloric acid medium (a) top view of 5-BTCA (b) top view of 5-BTCAH$^+$ (c) Side view of 5-BTCA (d) side view of BTCAH$^+$.

A comparison of the two modelled inhibitors as shown in Table 5 illustrates that both protonated and unprotonated forms show strong, spontaneous adsorption, but the protonated form exhibits slightly more stable total and adsorption energies, suggesting better corrosion inhibition potential under acidic conditions (Singh *et al.* 2019, Arrousse *et al.* 2022). The iron surface's strong interactions with thiophene, hydronium, and chloride ions may affect inhibition mechanisms, although competitive adsorption could reduce durability. Both forms undergo similar structural deformation upon adsorption, indicating good stability. These Monte Carlo and DFT results confirm effective adsorption of 5-BTCA, particularly when protonated, supporting its use as a corrosion inhibitor by forming stable protective films and interacting with competing species in corrosive environments, warranting further industrial application exploration (Singh *et al.* 2019, Arrousse *et al.* 2022).

**Mechanism of the corrosion inhibitor:** The corrosion inhibition mechanism of 5-BTCA on the Fe(110) surface is elucidated through a combination of NBO analysis, MESP mapping, frontier molecular orbital descriptors, and Monte Carlo simulations. NBO analysis reveals substantial donor–acceptor interactions within the molecule, with notably high second-order perturbation energies ($E^2$), particularly for $\pi \rightarrow \pi^*$ transitions such as $\pi C_1–C_2$ to $\pi C_3–C_4$, reaching up to 120.35 kcal/mol in the gas phase. These large stabilization energies reflect strong intramolecular conjugation, indicating significant electronic delocalization and enhanced charge transfer ability, key factors that promote effective chemisorption onto metal surfaces. Supporting these findings, the MESP surface highlights electron-rich regions around the carbonyl oxygen and thiophene ring, depicted as red zones, which serve as likely sites for interaction with the electron-deficient iron surface. This electrostatic complementarity suggests that adsorption involves both chemical and physical interactions.

Frontier molecular orbital analysis further emphasizes the molecule's reactivity: the HOMO energies ranging between –6.82 and –7.04 eV demonstrate strong electron-donating capacity, while a $E_g$ gap of 4.55–4.63 eV indicates moderate chemical reactivity. Additionally, the measured dipole moments and electrophilicity indices underscore the molecule's polar nature, favoring stable adsorption onto Fe(110), consistent with a chemisorption-driven mechanism.

Monte Carlo simulations quantify the interaction strength, yielding highly negative adsorption energies for both protonated (–74.31 kcal/mol) and

unprotonated (–86.17 kcal/mol) species—values far exceeding typical physisorption thresholds (–10 to –40 kcal/mol). This confirms that 5-BTCA adsorbs predominantly through strong chemisorption, likely involving coordinate or covalent bond formation with the iron surface. Such strong binding affinities align with the charge transfer capabilities suggested by NBO and orbital analyses. Therefore, 5-BTCA inhibits iron corrosion mainly via chemisorption characterized by robust orbital interactions and high adsorption energies. However, the existence of electron-rich electrostatic sites also implies a minor contribution from physisorption, indicating a mixed-mode adsorption mechanism with chemisorption as the dominant process.

**Conclusion**

This study provides a complete theoretical analysis of 5-bromothiophene-2-carbaldehyde (5-BTCA) as a corrosion inhibitor using Density Functional Theory (DFT) and Monte Carlo (MC) simulations. The obtained results show that 5-BTCA's inhibitory efficiency arises from its π-electron interactions, donor-acceptor charge transfer, and solvent-induced intramolecular stabilization. The HOMO-LUMO gaps (4.551 eV in water, 4.567 eV in ethanol) indicate high reactivity, promoting efficient electron transfer to the metal surface. The electrophilicity index (ω = 4.714 eV) and negative chemical potential (μ = −4.633 eV) further support its adsorption ability. MC simulations reveal both protonated and unprotonated forms adsorb favourably, with the protonated species exhibiting slightly stronger and more stable binding. NBO analysis confirms π-electron delocalization and lone-pair interactions stabilize the inhibitor-metal complex, while Molecular Electrostatic Potential (MEPS) maps illustrate solvent polarity's effect on charge distribution and adsorption behaviour. Overall, 5-BTCA demonstrates strong potential as a sustainable corrosion inhibitor in aqueous and acidic media and guides the design of enhanced thiophene-based inhibitors.

**References**

Akinyele, O. F., Adekunle, A. S., Olayanju, D. S., Oyeneyin, O. E., Durodola, S. S., Ojo, N. D., Akinmuyisitan, A. A., Ajayeoba, T. A. and Olasunkanmi, L. O. (2022). "Synthesis and corrosion inhibition studies of (E)-3-(2-(4-chloro-2-nitrophenyl) diazenyl)-1-nitrosonaphthalen-2-ol on Mild Steel dissolution in 0.5 M HCl solution-experimental, DFT and Monte Carlo simulations." Journal of Molecular Structure 1268: 133738. https://doi.org/10.1016/j.molstruc.2022.133738
.

Akrom, M. (2024). "Green corrosion inhibitors for iron alloys: a comprehensive review of integrating data-driven forecasting, density functional theory simulations, and experimental investigation." *Journal of Multiscale Materials* Informatics 1(1): 22-37. https://doi.org/10.62411/jimat.v1i1.10495.

Al-Amiery, A. A., Isahak, W. N. R. W. and Al-Azzawi, W. K. (2023). "Corrosion inhibitors: natural and synthetic organic inhibitors." *Lubricants* 11(4): 174. https://doi.org/10.3390/lubricants11040174.

Al-Amiery, A. A., Nik, W. M. N. W., Mohd, M. S., Ghazali, E. Y., Isahak, W., Khalid, W., Al-Azzawi, M. F. R. Z., Daoudi, W. and Dhande, I. O. V. A. Y. (2024). "Recent innovations in organic inhibitors for mild steel in corrosive solutions: A mini Review." *Journal of Sustainability Science and Management* 19(5): 146-173. https://doi.org/10.46754/jssm.2024.05.009.

Aliofkhazraei, M. (2018). "Corrosion inhibitors, principles and recent applications." https://doi.org/10.5772/intechopen.72943.

Arrousse, N., Fernine, Y., Al-Zaqri, N., Boshaala, A., Ech-Chihbi, E., Salim, R., El Hajjaji, F., Alami, A., Touhami, M. E. and Taleb, M. (2022). "Thiophene derivatives as corrosion inhibitors for 2024-T3 aluminum alloy in hydrochloric acid medium." *RSC advances* 12(17): 10321-10335. https://doi.org/10.1039/D2RA00185C.

Badeji, A. A., Omoniyi, M. T., Ogunbayo, T. B., Oladipo, S. D. and Akinbulu, I. A. (2024). "Quantum chemical investigation of the degradation of acid orange 7 by different oxidants." Discover Chemistry 1(1): 55. https://doi.org/10.1007/s44371-024-00059-x.Becke, A. D. (1993). "A new mixing of Hartree-Fock and local density-functional theories." Journal of chemical Physics 98(2): 1372-1377. https://doi.org/10.1063/1.464304.

Dunning Jr, T. H. (1989). "Gaussian basis sets for use in correlated molecular calculations. I. The atoms boron through neon and hydrogen." *The Journal of chemical physics* 90(2): 1007-1023. https://doi.org/10.1063/1.456153.

Frisch, M., Trucks, G., Schlegel, H., Scuseria, G., Robb, M., Cheeseman, J., Scalmani, G., Barone, V., Petersson, G., and Nakatsuji, H. (2016). "Gaussian 16 rev. C. 01, wallingford, ct. Wallingford, CT.".

Fukui, K. (1981). "The path of chemical reactions-the IRC approach." Accounts of chemical research

14(12): 363-368. https://doi.org/10.1021/ar00072a001.

Fukui, K., Yonezawa, T. and Shingu, H. (1952). "A molecular orbital theory of reactivity in aromatic hydrocarbons." *The Journal of Chemical Physics* 20(4): 722-725. https://doi.org/10.1063/1.1700523.

Gaber, G. A., Soliman, M. M., Nasr, Z. A. and Hyba, A. M. (2024). "Comprehensive investigation of sustainable corrosion inhibitors on Cu–Zn alloy in simulated cooling water: Electrochemical explorations, SEM/EDX analysis, and DFT/molecular simulations utilizing expired Bepotastine-B as a green inhibitor." *Sustainable Chemistry and Pharmacy* 37: 101340. https://doi.org/10.1016/j.scp.2023.101340.

Gadre, S. R., Suresh, C. H. and Mohan, N. (2021). "Electrostatic potential topology for probing molecular structure, bonding and reactivity." Molecules 26(11): 3289. https://doi.org/10.3390/molecules26113289.

Gece, G. (2008). "The use of quantum chemical methods in corrosion inhibitor studies." *Corrosion science* 50(11): 2981-2992. 10.1016/j.corsci.2008.08.043.

Guo, L., Safi, Z. S., Kaya, S., Shi, W., Tüzün, B., Altunay, N. and Kaya, C. (2018). "Anticorrosive effects of some thiophene derivatives against the corrosion of iron: a computational study." *Frontiers in chemistry* 6: 155. https://doi.org/10.3389/fchem.2018.00155.

Hansen, K. (2018). Molecular Dynamics and Monte Carlo Simulations. Statistical Physics of Nanoparticles in the Gas Phase, Springer: 253-285.

Hasanzadeh, N. (2024). "Theoretical Study of the Solvent Effect on Elimination Reactions: Hybrid-DFT Study and NBO Analysis." *Journal of Structural Chemistry* 65(5): 929-945. https://doi.org/10.1134/S002247662405007X.

Huang, Y., Rong, C., Zhang, R. and Liu, S. (2017). "Evaluating frontier orbital energy and HOMO/LUMO gap with descriptors from density functional reactivity theory." *Journal of molecular modeling* 23(1): 3. https://doi.org/10.1007/s00894-016-3175-x.

Kumar, V. S., Satya Narayana, T. V. V., Vijayakumar, P., Babu, V. R., Pavani, G., Swami, K. N. S. a. and Dr. Somarouthu, V. G. V. A. P. (2024). "Advances in Computational Quantum Chemistry: Methods, Applications, and Future Directions." J*ournal of Systems Engineering and Electronic* 34(5): 204-212.

Liu, L., Miao, L., Li, L., Li, F., Lu, Y., Shang, Z. and Chen, J. (2018). "Molecular electrostatic potential: a new tool to predict the lithiation process of organic battery materials." *The Journal of Physical Chemistry Letters* 9(13): 3573-3579. https://doi.org/10.1021/acs.jpclett.8b01123.

Mahmood, E. A., Poor Heravi, M. R., Khanmohammadi, A., Mohammadi-Aghdam, S., Ebadi, A. G. and Habibzadeh, S. (2022). "DFT calculations, structural analysis, solvent effects, and non-covalent interaction study on the para-aminosalicylic acid complex as a tuberculosis drug: AIM, NBO, and NMR analyses." *Journal of Molecular Modelin*g 28(10): 297. https://doi.org/10.1007/s00894-022-05279-5.

Marenich, A. V., Cramer, C. J. and Truhlar, D. G. (2009). "Universal solvation model based on solute electron density and on a continuum model of the solvent defined by the bulk dielectric constant and atomic surface tensions." The *Journal of Physical Chemistry* B 113(18): 6378-6396. https://doi.org/10.1021/jp810292n.

Mouats, N., Djellali, S., Ferkous, H., Sedik, A., Delimi, A., Boublia, A., Rachedi, K. O., Berredjem, M., Cukurovali, A. and Alam, M. (2024). "Comprehensive investigation of the adsorption, corrosion inhibitory properties, and quantum calculations for 2-(2, 4, 5-Trimethoxybenzylidene) hydrazine carbothioamide in mitigating corrosion of XC38 carbon steel under HCl environment." ACS omega 9(26): 27945-27962. https://doi.org/10.1021/acsomega.3c10240.

Neyts, E. C. and Bogaerts, A. (2012). Combining molecular dynamics with Monte Carlo simulations: implementations and applications. Theoretical chemistry in Belgium: a topical collection from theoretical chemistry accounts, Springer: 277-288.

Nyquist, R. A. (1986). "Factors affecting infrared group frequencies: Carbonyl stretching absorption bands." *Applied spectroscopy* 40(3): 336-339.

Oladipo, S. D., Luckay, R. C., Badeji, A. A., Zamisa, S. Z., Olalekan, S. O. and Oladoye, P. O. (2025). "Structural studies, DFT computational analysis and inhibitory potential of (E)-N'-(2-bromophenyl)-N-(2, 6-diisopropylphenyl) formamidine against CDK1 and CDK2." *Journal of Molecular Structure* 1320: 139734. https://doi.org/10.1016/j.molstruc.2024.139734.

Oladipo, S. D., Zamisa, S. J., Badeji, A. A., Ejalonibu, M. A., Adeleke, A. A., Lawal, I. A., Henni, A. and Lawal, M. M. (2023). "Ni2+ and Cu2+ complexes of

N-(2, 6-dichlorophenyl)-N-mesityl formamidine dithiocarbamate structural and functional properties as CYP3A4 potential substrates." *Scientific Reports* 13(1): 13414. https://doi.org/10.1038/s41598-023-39502-x.

Oyeneyin, O. E., Ibrahim, A., Ipinloju, N., Ademoyegun, A. J. and Ojo, N. D. (2024). "Insight into the corrosion inhibiting potential and anticancer activity of 1-(4-methoxyphenyl)-5-methyl-N'-(2-oxoindolin-3-ylidene)-1H-1, 2, 3-triazole-4-carbohydrazide via computational approaches." *Journal of Biomolecular Structure and Dynamics* 42(20): 11149-11166. https://doi.org/10.1080/07391102.2023.2260491.

Oyeneyin, O. E., Ojo, N. D., Ipinloju, N., Agbaffa, E. B. and Emmanuel, A. V. (2022). "Investigation of the corrosion inhibition potentials of some 2-(4-(substituted) arylidene)-1H-indene-1, 3-dione derivatives: density functional theory and molecular dynamics simulation." *Beni-Suef University Journal of Basic and Applied Sciences* 11(1): 132. https://doi.org/10.1186/s43088-022-00313-0.

Popoola, L., Grema, A., Latinwo, G., Gutti, B. and Balogun, A. (2013). "Corrosion problems during oil and gas production and its mitigation." *International Journal of Industrial Chemistry* 4(1): 35. https://doi.org/10.1186/2228-5547-4-35.

Prasad, A. R., Kunyankandy, A. and Joseph, A. (2020). "Corrosion inhibition in oil and gas industry: Economic considerations." Corrosion inhibitors in the oil and gas industry: 135-150. https://doi.org/10.1002/9783527822140.ch5.

Resen, A. M., Jasim, A. N., Qasim, H. S., Hanoon, M. M., Al-Kaabi, M. H., Al-Amiery, A. A. and Al-Azzawi, W. K. (2023). "A combined experimental and theoretical study of a novel corrosion inhibitor derived from thiophen." Carbon Neutralization 2(6): 661-677. https://doi.org/10.1002/cnl2.92.

Roscher, J., Liu, D., Xie, X. and Holze, R. (2024). "Comparative Assessment of Aromatic Iron Corrosion Inhibitors with Electrochemical Methods." Corrosion and Materials Degradation 5(4): 593-600. https://doi.org/10.3390/cmd5040024.

Šebek, J. í., Knaanie, R., Albee, B., Potma, E. O. and Gerber, R. B. (2013). "Spectroscopy of the C–H stretching vibrational band in selected organic molecules." The Journal of Physical Chemistry A 117(32): 7442-7452. https://doi.org/10.1021/jp4014674.

Shaker, L., Al-Amiery, A., Al-Hamid, M. and Al-Azzawi, W. (2024). "Understanding the mechanism of organic corrosion inhibitors through density functional theory." Koroze a Ochrana Materiálu 68(1): 9-21. https://doi.org/10.2478/kom-2024-0002.

Shankar, U., Gogoi, R., Sethi, S. K. and Verma, A. (2022). Introduction to materials studio software for the atomistic-scale simulations. Forcefields for atomistic-scale simulations: *materials and applications, Springer:* 299-313.

Sheryazov, S., Sarkulova, Z. S., Balgynova, A., Shukirova, S. and Zh, T. A. (2024). "METHODS OF CORROSION PROTECTION OF EQUIPMENT AND PIPELINES IN THE OIL AND GAS INDUSTRY." Научный журнал" Вестник Актюбинского регионального университета имени К. Жубанова" 76(2): 35-42. https://doi.org/10.70239/arsu.2024.t76.n2.05.

Singh, A., Ansari, K. R., Quraishi, M. A. and Lin, Y. (2019). Investigation of corrosion inhibitors adsorption on metals using density functional theory and molecular dynamics simulation. Corrosion Inhibitors, IntechOpen.

Suresh, C. H., Remya, G. S. and Anjalikrishna, P. K. (2022). "Molecular electrostatic potential analysis: A powerful tool to interpret and predict chemical reactivity." Wiley Interdisciplinary Reviews: *Computational Molecular Science* 12(5): e1601. https://doi.org/10.1002/wcms.1601.

Ueda, W. (2022). Crystalline Metal Oxide Catalysts, Springer.

Verma, C., Ebenso, E. E. and Quraishi, M. (2017). "Ionic liquids as green and sustainable corrosion inhibitors for metals and alloys: an overview." J*ournal of Molecular Liquids* 233: 403-414. 10.1016/j.molliq.2017.02.111.

Wilson, A. K., Woon, D. E., Peterson, K. A. and Dunning Jr, T. H. (1999). "Gaussian basis sets for use in correlated molecular calculations. IX. The atoms gallium through krypton." The Journal of chemical physics 110(16): 7667-7676. https://doi.org/10.1063/1.478678.

Zhan, C.-G., Nichols, J. A. and Dixon, D. A. (2003). "Ionization potential, electron affinity, electronegativity, hardness, and electron excitation energy: molecular properties from density functional theory orbital energies." The *Journal of Physical Chemistry* A 107(20): 4184-4195. https://doi.org/10.1021/jp0225774.

Zhao, Y., Schultz, N. E. and Truhlar, D. G. (2005). "Exchange-correlation functional with broad accuracy for metallic and nonmetallic compounds, kinetics, and noncovalent interactions." The Journal of chemical physics 123(16). https://doi.org/10.1063/1.2126975.